

# PROBING CHIRAL SYMMETRY RESTORATION WITH HEAVY IONS \*

JOCHEN WAMBACH

Institut für Kernphysik  
Technische Universität Darmstadt  
Schloßgartenstr. 9  
D-64289, Darmstadt, Germany

RALF RAPP

Department of Physics and Astronomy  
State University of New York at Stony Brook  
Stony Brook, NY 11794-3800, U.S.A.

*(Received August 11, 2018)*

It is discussed how chiral symmetry restoration manifests itself through mixing of vector and axial-vector correlators. The vector correlator is directly accessible in relativistic heavy-ion collisions. Within models of the vector correlator its implications for low-mass dilepton spectra are reviewed.

## 1. Introduction

The goal of ultra-relativistic heavy-ion collisions is to create new states of hadronic matter that are believed to have existed until a few tens of microseconds after the 'big bang'. These efforts were largely stimulated by lattice QCD predictions that hadronic matter at high energy density undergoes a phase transition to a plasma of deconfined quarks and gluons. At present the lattice calculations with realistic light quark masses yield a transition temperature  $T_c = 150 \pm 20$  MeV [1] at which there is a rapid increase of the thermodynamic quantities such as energy- and entropy density. The transition is accompanied by a restoration of chiral symmetry, signaled by a sharp decrease of the chiral condensate,  $\langle \bar{q}q \rangle_T$ , near  $T_c$ .

---

\* Presented at the International Workshop on 'The Structure of Mesons, Baryons, and Nuclei' on the occasion of Josef Speth's 60th birthday

In the following, we shall concentrate on the chiral symmetry aspects of the phase transition and potential signals in heavy-ion collisions. In the physical vacuum chiral symmetry is spontaneously broken. For the light meson spectrum this manifests itself in two ways: (i) the appearance of (nearly) massless Goldstone bosons (pion, kaon, eta) which interact weakly at low energies, and (ii) the absence of parity doublets, *i.e.* the splitting of scalar- and pseudoscalar, as well as vector and axial-vector mesons. For the following discussion property (ii) will be most important. Given the vector and axial-vector currents ( $N_f = 2$ ),

$$V_\mu^a = \bar{q}\gamma_\mu(\tau^a/2)q, \quad A_\mu^a = \bar{q}\gamma_\mu\gamma_5(\tau^a/2)q, \quad (1)$$

the vacuum properties of the vector and axial-vector mesons are encoded in the corresponding correlators

$$\begin{aligned} \langle V_\mu^a(x)V_\nu^b(0) \rangle &= -\frac{\delta^{ab}}{\pi} \int d^4q \theta(q^0) e^{iqx} \text{Im}\Pi_{\mu\nu}^V(q) \\ \langle A_\mu^a(x)A_\nu^b(0) \rangle &= -\frac{\delta^{ab}}{\pi} \int d^4q \theta(q^0) e^{iqx} \left( \text{Im}\Pi_{\mu\nu}^A(q) - F_\pi^2 \delta(q^2) q_\mu q_\nu \right) \end{aligned} \quad (2)$$

Note the explicit contribution of the pion to the axial-vector correlator through the pion weak decay constant,  $F_\pi$ . Current conservation implies a four-dimensionally transverse tensor structure

$$\Pi_{\mu\nu}^{V,A}(q) = \left( g_{\mu\nu} - \frac{q_\mu q_\nu}{q^2} \right) \Pi^{V,A}(s), \quad \Pi^{V,A}(s) = \frac{1}{3} g^{\mu\nu} \Pi_{\mu\nu}^{V,A}(q), \quad (3)$$

where  $s = q^2$ . The isovector part of the spectral function  $\text{Im}\Pi^V$  is observed from the hadronic part of the  $e^+ + e^- \rightarrow \text{even } \pi$  which has a sharp resonance corresponding to the  $\rho$ -meson (770 MeV). On the other hand, the isovector part of  $\text{Im}\Pi^A$  can be observed from the hadronic part of the decay  $\tau \rightarrow \text{odd } \pi$ . This part has a broad  $a_1$  peak (1260 MeV). The two spectral functions are clearly different which is one of the experimental signatures that chiral symmetry is spontaneously broken. The degree of symmetry breaking follows from the Weinberg sum rule [2]

$$\frac{1}{\pi} \int \frac{ds}{s} \left( \text{Im}\Pi^V(s) - \text{Im}\Pi^A(s) \right) = F_\pi^2. \quad (4)$$

Physically it states that the difference in vector and axial-vector polarizabilities  $\Pi_{\mu\mu}^V(0) - \Pi_{\mu\mu}^A(0)$  of the QCD vacuum is given by the order parameter of spontaneous symmetry breaking. A second sum rule can be derived

$$\frac{1}{\pi} \int ds \left( \text{Im}\Pi^V(s) - \text{Im}\Pi^A(s) \right) = 0, \quad (5)$$

which implies that the 'energy weighted' sum rules (EWSR) of the two spectral functions are identical. This is a well-known consequence of the conservation of vector and axial-vector currents in the chiral limit.

## 2. How to Detect Symmetry Restoration?

In the experimental study of chiral restoration in heavy-ion collisions the change in the quark condensate  $\langle \bar{q}q \rangle_{\mu, T}$  is not directly measurable. However, it follows from chiral symmetry alone that, at the phase boundary, the scalar and pseudo-scalar correlators as well as the vector and axial-vector correlators must become identical. In principle, the observation of parity mixing can thus serve as a unique signal for chiral restoration. Since the vector and axial-vector correlators in the vacuum are largely saturated by narrow resonances, the objective is then to study the spectral changes of these 'collective modes' as a function of  $\mu$  and  $T$ .

The vector correlator is directly accessible in heavy-ion collisions since it couples to photons or dileptons both of which undergo negligible final-state interaction. Concerning the spectral properties there are, in principle, two possibilities: (1) the vector modes could become 'soft' at the phase boundary giving rise to 'dropping masses'. This is the hypothesis of 'Brown-Rho scaling' [3] and would be a natural consequence of a direct relationship between masses and the chiral condensate, as found in the vacuum. It explains qualitatively the rapid increase in entropy density across the phase boundary, as is seen in lattice QCD [4]; (2) the vector mesons remain massive, becoming degenerate with their axial partners. To elucidate this possibility further the properties of the in-medium correlators need to be discussed in more detail.

## 3. In-Medium Vector and Axial-Vector Correlators

In equilibrium, the finite-temperature (chemical potential) correlation functions are evaluated in the grand canonical ensemble,

$$\tilde{\Pi}_{\mu\nu}^V(q_0, \vec{q}) = i\delta^{ab} \int d^4x e^{iq \cdot x} \rho_i \langle i|V_\mu^a(x)V_\nu^b(0)|i \rangle, \quad (6)$$

and a similar expression for  $\tilde{\Pi}_{\mu\nu}^A(q_0, \vec{q})$  ( $\rho_i$  is the usual density matrix). Specification of a matter rest frame implies that Lorentz invariance is broken. Thus the momentum-space correlators  $\tilde{\Pi}_{\mu\nu}^{V,A}$  will depend on energy and three-momentum separately and not on just their invariant  $q$ . Also, the

number of Lorentz tensors is larger. Introducing longitudinal and transverse projection tensors  $P_{\mu\nu}^{L,T}$  one has

$$\tilde{\Pi}_{\mu\nu}^{V,A}(q_0, \vec{q}) = \tilde{\Pi}_L^{V,A} P_{\mu\nu}^L + \tilde{\Pi}_T^{V,A} P_{\mu\nu}^T, \quad (7)$$

which in vacuum reduces to eq. (3) with  $\Pi^{V,A} \equiv \Pi_L^{V,A} = \Pi_T^{V,A}$ . The pion, being a massless Goldstone boson in the chiral limit, is special. It only contributes to the longitudinal axial correlator and, without loss of generality, can be subsumed in the axial-vector correlator.

The in-medium extensions of the Weinberg-sum rules (for  $\mu = 0$ ) have been derived in [5]. They read

$$\int_0^\infty \frac{dq_0}{q_0^2 - \vec{q}^2} q_0 \left( \text{Im} \tilde{\Pi}_L^V(q_0, \vec{q}) - \text{Im} \tilde{\Pi}_L^A(q_0, \vec{q}) \right) = 0 \quad (8)$$

and

$$\int_0^\infty dq_0 q_0 \left( \text{Im} \tilde{\Pi}_{L,T}^V(q_0, \vec{q}) - \text{Im} \tilde{\Pi}_{L,T}^A(q_0, \vec{q}) \right) = 0 \quad (9)$$

and hold at each value of the three-momentum  $\vec{q}$ . Note that the polarizability sum rule (8) only involves the longitudinal part of the spectral functions while the EWSR (9) holds for both parts separately. As usual in many-body physics, sum rules put important constraints on models of the spectral functions and can be used to gain insight into the role of in-medium effects. This can be illustrated most stringently in the case of vanishing baryo-chemical potential. In the chiral limit, the pion is massless below the critical temperature for chiral symmetry restoration and, in the low temperature limit, the heat bath is dominated by pions. It can be proven that in this limit the masses of the vector and axial-vector mesons do not change to order  $T^2$  [6]. To this order there are only changes in the couplings of the currents and the finite-temperature correlators are described by  $T$ -dependent mixing of the zero-temperature correlators

$$\begin{aligned} \tilde{\Pi}_{\mu\nu}^V(q_0, \vec{q}) &= (1 - \varepsilon) \Pi_{\mu\nu}^V(q) + \varepsilon \Pi_{\mu\nu}^A(q) \\ \tilde{\Pi}_{\mu\nu}^A(q_0, \vec{q}) &= (1 - \varepsilon) \Pi_{\mu\nu}^A(q) + \varepsilon \Pi_{\mu\nu}^V(q). \end{aligned} \quad (10)$$

To order  $T^2$ ,  $\varepsilon \equiv T^2/6F_\pi^2$ , and therefore the temperature dependence of the pion decay constant is  $F_\pi^2(T) = (1 - \varepsilon)F_\pi^2$ , consistent with the results from chiral perturbation theory [7]. As is easily verified, the sum rules (8) and (9) are fulfilled. As the mixing becomes maximal,  $\varepsilon = 1/2$ , chiral symmetry is restored. The in-medium sum rules can be used to gain further insight into the behavior of the in-medium correlators. Restricting the discussion

to vanishing three-momentum for simplicity and resonance saturation in the vacuum through the current-field identities

$$V_\mu^a = \frac{m_\rho^2}{g_\rho} \rho_\mu^a, \quad A_\mu^a = \frac{m_{a_1}^2}{g_{a_1}} a_\mu^a + \text{pion}, \quad (11)$$

we obtain for the vector spectral density in the  $\rho$ -meson channel

$$\pi \text{Im} \tilde{\Pi}_L^\rho(q_0) = \frac{m_\rho^4}{g_\rho^2} \text{Im} \frac{1}{q_0^2 - m_\rho^2 - \Sigma_\rho(q_0)}, \quad (12)$$

where  $\Sigma_\rho$  denotes the  $\rho$ -meson selfenergy at finite temperature. A narrow width approximation,  $\text{Im} \Sigma_\rho \ll m_\rho^{*2}$ , yields

$$\pi \text{Im} \tilde{\Pi}_L^\rho(q_0) = \frac{m_\rho^4}{g_\rho^2} \delta(q_0^2 - m_\rho^2 - \text{Re} \Sigma_\rho(q_0)). \quad (13)$$

The pole mass is determined from  $m_\rho^{*2} = m_\rho^2 + \text{Re} \Sigma_\rho(m_\rho^*)$  and the spectral density can be written as

$$\pi \text{Im} \tilde{\Pi}_L^\rho(q_0) = Z_\rho \frac{m_\rho^4}{g_\rho^2} \delta(q_0^2 - m_\rho^{*2}) \quad (14)$$

with a temperature-dependent residue. Similarly, for the axial-vector spectral density,

$$\pi \text{Im} \tilde{\Pi}_L^{a_1}(q_0) = Z_{a_1} \frac{m_{a_1}^4}{g_{a_1}^2} \delta(q_0^2 - m_{a_1}^{*2}) + Z_\pi F_\pi^2 q_0^2 \delta(q_0^2). \quad (15)$$

Inserting these spectral densities into the sum rules (8) and (9) implies that  $Z_\rho = Z_{a_1}$  and

$$Z_\pi = 2Z_\rho \left( \frac{m_\rho^2}{m_\rho^{*2}} - \frac{m_\rho^2}{m_{a_1}^{*2}} \right). \quad (16)$$

From the fact that the vector- and axial-vector spectral functions have to become identical at chiral restoration one expects in the narrow width approximation that  $m_{a_1}^* \rightarrow m_\rho^*$  as the phase transition is approached. As a result the residue at the pion pole,  $Z_\pi$ , has to vanish. Whether both  $m_\rho^*$  and  $m_{a_1}^*$  vanish at  $T_c$  or remain finite cannot be decided from sum rule arguments alone. To answer this question dynamical models have to be employed.

#### 4. Hadronic Models for the Vector Correlator

In modeling the in-medium vector and axial-vector correlators one should realize that, at SpS energies, the phase space in the final state is dominated by mesons (mostly pions) with a meson/baryon ratio of 5-7 [8]. An obvious starting point is therefore a pure pion gas. For the  $\rho$ -meson which, in the Vector-Dominance Model (VDM), couples predominantly to two-pion states this implies a modification of the pion loop through the heat bath as well as contributions from direct  $\rho - \pi$  scattering. The resulting thermal broadening has been calculated in various frameworks [9] and found to be rather small. A model-independent approach has been put forward by [10] which relies on a chiral reduction formalism in the virial expansion. Being an expansion in temperature, the in-medium vector correlator (6) can then be related to the vacuum vector- and axial-vector correlators in much the same way as discussed in the previous section. The vacuum spectral information is deduced from experiment.

In spite of the scarcity of baryons in the hot hadron gas, they have a significant impact on the spectral properties of vector mesons, largely because of strong meson-baryon coupling. When baryons are involved the mixing of vector- and axial-vector correlators is much more complicated than at  $\mu = 0$  and it has only started to be addressed recently [11]. Putting these difficulties aside, several approaches have been put forward to determine the in-medium vector correlator. In analogy to the virial expansion at finite temperature an obvious starting point is a combined low  $T$ , small  $\mu$  expansion of (6), resulting in the leading-order corrections to the vacuum correlators in both pion- and nucleon number density,  $n_\pi$  and  $n_N$  [10, 12]. To leading order in  $n_N$  the nucleon Compton amplitude enters which is constrained from  $\gamma N$  photoabsorption data and the nucleon polarizabilities. In [12] the nucleon Compton tensor is evaluated in the VDM combined with chiral  $SU(3)$  dynamics, based on an effective meson-baryon Lagrangian. The calculation reveals that the  $\rho$ -meson suffers substantial broadening, as density increases. The position of the 'pole mass' is hardly affected, however.

A second approach for the in-medium spectral properties of the  $\rho$ -meson starts from the well-known observation that pion propagation in the nucleus is strongly modified. A wealth of elastic  $\pi$ -nucleus scattering data has provided detailed understanding of the relevant physical mechanisms [13]. The dominant contributions originate from  $P$ -wave  $\pi N$  scattering through  $N$ -hole and  $\Delta$ -hole loops, giving rise to a momentum-softening of the pion dispersion relation. In the VDM it is therefore natural to account for this effect by replacing the vacuum two-pion loop with in-medium pions [14]. Gauge invariance is ensured by including appropriate vertex corrections. To lowest order in nucleon density this approach represents a pion cloud model

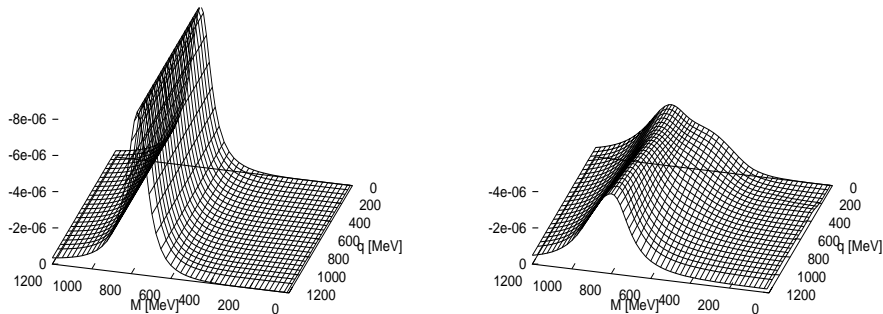


Fig. 1.  $\rho$ -meson spectral function versus invariant mass  $M$  and 3-momentum  $q$  in vacuum (left panel) and in normal nuclear matter (right panel).

for the nucleon Compton amplitude which largely coincides with that of [10] and [12]. In addition to leading-order contributions in  $n_N$  there naturally emerge higher orders in density, most notably  $n_N^2$  terms. These correspond to two-nucleon processes of meson-exchange character and  $NN$ - and  $N\Delta$ -bremsstrahlung contributions. Besides the medium modifications caused by dressing the intermediate 2-pion states, direct interactions of the  $\rho$ -meson with surrounding nucleons in the gas have to be considered. Indeed, there are several well-established resonances in the particle data table [15] which strongly couple to the  $\rho N$  decay channel, e.g. the  $N(1720)$  and the  $\Delta(1905)$ . This led to the suggestion [16] to consider  $P$ -wave particle-hole excitations of the type  $\rho N(1720)N^{-1}$  and  $\rho\Delta(1905)N^{-1}$ . In a more complete description other resonances with appreciable  $\rho N$  widths have been included [17, 18], most notably  $S$ -wave excitations into  $N(1520)$ ,  $\Delta(1700)$ , etc.. The most simple version of the VDM tends to overestimate the  $B^* \rightarrow N\gamma$  branching fractions when using the hadronic coupling constants deduced from the  $B^* \rightarrow N\rho$  partial widths. This is corrected for by employing an improved version of the VDM [19], which allows to adjust the  $B^*N\gamma$  coupling independently.

Combining the effects of pionic modifications and resonant  $\rho N$  scattering, the resulting  $\rho$ -meson spectral functions  $\text{Im}\tilde{\Pi}^\rho = 1/3(\text{Im}\tilde{\Pi}_L^\rho + 2\text{Im}\tilde{\Pi}_T^\rho)$  are displayed in Fig. 1. One observes significant broadening especially at small  $\vec{q}$  with a low-mass shoulder which originates from intermediate  $\Delta N^{-1}\pi$  states and resonant  $N(1520)N^{-1}$  excitations. As  $\vec{q}$  increases the shoulder moves towards the  $M = 0$  line which can be understood from simple kinematics.

An important constraint for models of in-medium  $\rho$ -meson propagation is photoabsorption on nucleons and nuclei, for which a wealth of data exist over a wide range of energies. Real photons correspond to the  $M = 0$

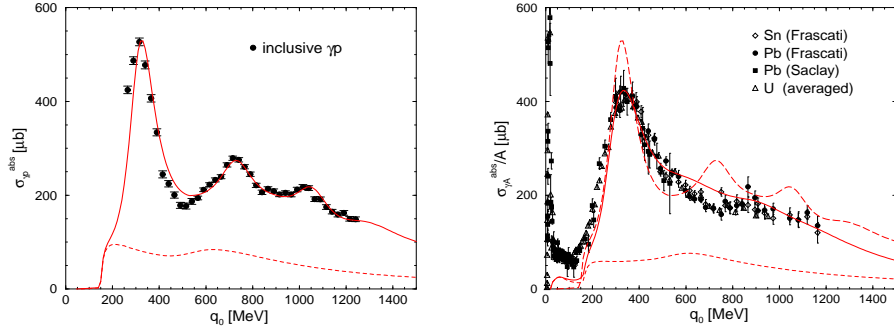


Fig. 2. The photoabsorption spectrum on the proton [20] (left panel) and on nuclei [21] (right panel). The solid lines are the full results in the low-density limit (left panel) and for  $\rho_N = 0.8\rho_0$  (right panel), and short-dashed lines indicate the non-resonant background contributions; the results are taken from [22].

line in the right panel of Fig. 1. Within the model discussed above, the total photoabsorption cross section per nucleon can be calculated straightforwardly [18]. Taking the low-density limit,  $n_N \rightarrow 0$ , only terms linear in density contribute, representing the absorption process on a single nucleon. Adjusting the model parameters to optimally reproduce the  $\gamma p$  data yields results displayed in the left panel of Fig. 2. Photoabsorption on nuclei can be reproduced with similar quality (right panel of Fig. 2). It is noteworthy that, in the nucleus, strength below  $m_\pi$  is obtained which originates from two-nucleon processes via meson-exchange currents and is nothing but the ‘quasi-deuteron tail’ of the giant dipole resonance.

Another model constraint can be obtained from the analysis of  $\pi N \rightarrow \rho N$  production [23] which is in fact dominated by pion cloud contributions (rather than  $B^*$  resonances). This imposes stringent constraints on the hadronic form factor at the  $\pi NN$  vertex (requiring  $\Lambda_{\pi NN} \simeq 300-400$  MeV), which are included in the results shown in Figs. 1-3 [22, 24].

## 5. Comparison with Dilepton Data

Including the above mentioned hadronic model constraints gives confidence in extrapolations to the time-like region of dilepton production. For  $\pi\pi$ -annihilation/ $\rho$ -meson decays the in-medium dilepton rate is obtained as

$$\frac{dN_{\pi^+\pi^-\rightarrow l+l^-}}{d^4x d^4q} = -\frac{\alpha^2}{3\pi^3} \frac{f^\rho(q_0; T)}{M^2} g^{\mu\nu} \text{Im}\tilde{\Pi}_{\mu\nu}^\rho(q_0, \vec{q}). \quad (17)$$

In the model of [22, 25] most of the important processes discussed above have been included such that the  $\rho$ -meson propagator contains aside from



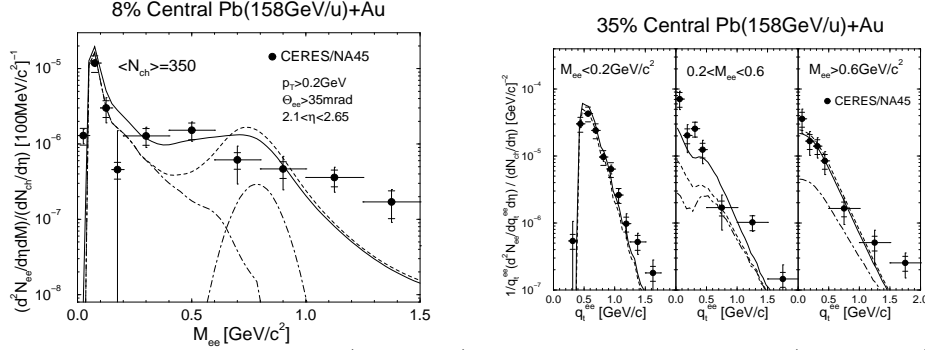


Fig. 3. Dilepton invariant mass (left panel) and transverse momentum (right panel) spectra in Pb+Au collisions at CERN-SpS energies [28]. The dashed-dotted lines arise from hadron decays after freezeout [28, 27]; adding the contribution from  $\pi^+\pi^-$  annihilation in the hadronic fireball, one obtains the dashed lines (when using the free  $\rho$  propagator) or the full lines (when using the in-medium  $\rho$  propagator); the results are taken from [22].

the nucleonic contributions also some parts from the pion/kaon gas.

To compare the theoretical rates with data, the space-time history of the heavy-ion collision has to be specified. There are several possibilities for modeling the collision. Within a simple 'fireball' model [26, 25] initial conditions in temperature and hadron abundances are taken from transport model calculations; assuming local thermal equilibrium as well as chemical equilibrium, the space-time history is then determined by a simple cooling curve,  $T(t)$ , from some initial time,  $t_i$ , up to the 'freeze-out time',  $t_f$ . For SpS energies such cooling curves are available from transport theory [27] and can be easily parameterized. The time evolution of the hadron abundances is determined by chemical equilibrium and agrees well with the transport model results. The observed spectrum is then obtained by integrating the 'local rate' (17) in time, accounting for the detector acceptance in addition, cp. Fig. 3. When including the in-medium effects due to hadronic rescattering as discussed above, reasonable agreement is obtained (full curves) with both the invariant mass (left panel) and transverse momentum spectra (right panel). Note that the major part of the enhancement for  $0.2 \text{ GeV} < M_{ee} < 0.6 \text{ GeV}$  is correctly ascribed to rather small pair momenta  $q_t \leq 0.7 \text{ GeV}$ . This might in fact resolve the question why the  $\mu^+\mu^-$  spectra measured by the NA50 collaboration show a much less pronounced excess at low  $M_{\mu\mu}$ : their transverse momentum cut of  $p_t > 1 \text{ GeV}$  will eliminate most of enhancement generated within the model.

The fireball model is rather crude and does not incorporate detailed flow dynamics. A more sophisticated description is provided by hydrodynamical

simulations. In this case the 'local rates' (17) refer to a given fluid cell and can be directly implemented. So far, however, no results are available.

A third way is to supply transport calculations with rates obtained from in-medium vector-meson propagation. For the  $\rho$ -meson these have been implemented in simulations using the *HSD* model for the transport [29]. The results are very similar to the ones of Fig. 3 obtained in the fireball model.

## 6. Summary

Recent theoretical efforts in understanding the nature of chiral symmetry restoration at finite temperature and baryochemical potential and their implications for low-mass dilepton production in URHIC's have been discussed. Special emphasis has been put on the in-medium Weinberg sum rules and their implications for the mixing of vector and axial-vector correlators. A unique signal for chiral symmetry restoration in URHIC's would be the observation of such a mixing. It strictly follows from chiral symmetry but is difficult to detect. Only the vector correlator is accessible via electromagnetic probes.

Meanwhile, the development of hadronic models for in-medium properties of vector mesons has advanced to a more quantitative level, in particular owing to phenomenological constraints inferred e.g. from photoabsorption data. Thus, trustworthy calculations for dilepton production in hot/dense matter can be performed. While some approaches inherently involve constraints from chiral symmetry [12, 10], others lack an obvious connection to chiral symmetry emphasizing, however, input from hadronic phenomenology [26, 25, 18]. When supplemented by models for the space-time history of the heavy-ion collision dynamics, reasonable theoretical account for the experimentally observed low-mass dilepton enhancement seems to emerge [25, 29, 22]. Further calculations addressing more exclusive observables as e.g. the recently measured transverse momentum spectra [28], where the major part of the low-mass enhancement has been identified at low pair- $p_t$ , also seem to be in line [22] with the data.

## Acknowledgments

This work was supported in part by the A.-v.-Humboldt foundation (within a Feodor-Lynen fellowship), the NSF under grant no. NSF-PHY-94-21309 and the US-DOE under grant no. DE-FG02-88ER40388.

## REFERENCES

- [1] E. Laermann, Nucl. Phys. **A610** (1996) 1c.
- [2] S. Weinberg, Phys. Rev. Lett **18** (1967) 507.
- [3] G.E. Brown and M. Rho, Phys. Rev. Lett **66** (1991) 2720.
- [4] F. Karsch, Nucl. Phys. **A590** (1995) 367c.
- [5] J.I. Kapusta and E.V. Shuryak, Phys. Rev. **D49** (1994) 4694.
- [6] V.L. Eletsky and B.L. Ioffe, Phys. Rev. **D51** (1995) 2371.
- [7] J. Gasser and H. Leutwyler, Phys. Lett **B184** (1987) 83.

- [8] J. Stachel, Nucl. Phys. **A610** (1996) 509c.
- [9] C. Gale and J. Kapusta, Nucl. Phys. **B357** (1991) 65; K. Haglin, Nucl. Phys. **A584** (1995) 719; C. Song and V. Koch, Phys. Rev. **C54** (1996) 3218.
- [10] J.V. Steele, H. Yamagishi and I.Zahed, Phys. Lett. **B384** (1996) 255; Phys. Rev. **D57** (1997) 5605.
- [11] G. Chanfray, J. Delorme and M. Ericson, nucl-th/9801020.
- [12] F. Klingl, N. Kaiser and W. Weise, Zeit. Phys. **A356** (1996) 193; Nucl. Phys. **A624** (1997) 527.
- [13] T.E.O Ericson and W. Weise, '*Pions and Nuclei*', Clarendon, Oxford 1988.
- [14] G. Chanfray and P. Schuck, Nucl. Phys. **A555** (1993) 329; M. Herrmann, B. Friman and W. Nörenberg, Nucl. Phys. **A560** (1993) 411; M. Asakawa, C. M. Ko, P. Lévai and X. J. Qiu, Phys. Rev. **C46** (1992) R1159.
- [15] Particle Data Group, R.M. Barnett et al., Phys. Rev. **D54** (1996) 1.
- [16] B. Friman and H.J. Pirner, Nucl. Phys. **A617** (1997) 496.
- [17] W. Peters, M. Post, H. Lenske, S. Leupold and U. Mosel, Nucl. Phys. **A632** (1998) 109.
- [18] R. Rapp, M. Urban, M. Buballa and J. Wambach, Phys. Lett. **B417** (1998) 1.
- [19] N.M. Kroll, T.D. Lee and B. Zumino, Phys. Rev. **157** (1967) 1376.
- [20] T.A. Armstrong et al., Phys. Rev. **D5** (1972) 1640.
- [21] A. Lepretre et al., Phys. Lett. **79B** (1978) 43; J. Ahrens, Nucl. Phys. **A446** (1985) 229c; J. Ahrens et al., Phys. Lett. **146B** (1984) 303; Th. Frommhold et al., Phys. Lett. **B295** (1992) 28 and Zeit. Phys. **A350** (1994) 249; N. Bianchi et al., Phys. Lett. **B299** (1993) 219 and Phys. Rev. **C54** (1996) 1688.
- [22] R. Rapp, Proc. of 33rd Recontres de Moriond on 'QCD and High Energy Hadronic Interactions', Les Arcs (France), March 21-28, 1998, Edition Frontiers, ed. J. Tran Thanh Van, and nucl-th/9804065.
- [23] B. Friman, Proc. of the APCTP workshop on Astro-Hadron Physics, Seoul (Korea), Oct. 25-31, 1997, and nucl-th/9801053.
- [24] T. Roth, M. Buballa, R. Rapp and J. Wambach, in preparation.
- [25] R. Rapp, G. Chanfray and J. Wambach, Nucl. Phys. **A617** (1997) 472.
- [26] G. Chanfray, R. Rapp and J. Wambach, Phys. Rev. Lett. **76** (1996) 368.
- [27] G.Q. Li, C.M. Ko, G.E. Brown and H. Sorge, Nucl. Phys. **A611** (1996) 539.
- [28] CERES/NA45 coll., G. Agakichiev *et al.*, Phys. Lett. **B422** (1998) 405; C. Voigt, PhD thesis, University of Heidelberg 1998.
- [29] W. Cassing, E.L. Bratkovskaya, R. Rapp and J. Wambach, Phys. Rev. **C57** (1998) 916.